# "Integration of Wind Solar Hybrid & Challenges to Grid Connectivity & It's Mitigation"

A.U.Moon
PG Student Abha Gaikwad Patil College of Engineering, Mohgaon,Wardha Road ,Nagpur India.

R.R Shaha
Head of Department (Electrical Engineering), Abha Gaikwad Patil College of Engineering, Mohgaon,Wardha Road, Nagpur India.

**Abstract – Environmentally friendly solutions are becoming more prominent than ever as a result of concern regarding the state of our deteriorating planet. This paper presents a new system configuration of the front-end rectifier stage for a hybrid wind/photovoltaic energy system. This configuration allows the two sources to supply the load separately or simultaneously depending on the availability of the energy sources. The inherent nature of this Cuk-SEPIC fused converter, additional input filters are not necessary to filter out high frequency harmonics. Harmonic content is detrimental for the generator lifespan, heating issues, and efficiency. The fused multiinput rectifier stage also allows Maximum Power Point Tracking (MPPT) to be used to extract maximum power from the wind and sun when it is available. An adaptive MPPT algorithm will be used for the wind system and a standard perturb and observe method will be used for the PV system. Operational analysis of the proposed system will be discussed in this paper. Simulation results are given to highlight the merits of the proposed circuit.**

**Index Terms – Hybrid system, CUK-SEPIC converter, renewable energy, photovoltaic system, wind power, Maximum power point tracking (MPPT).**

## 1. INTRODUCTION

With increasing concern of global warming and the depletion of fossil fuel reserves, many are looking at sustainable energy solutions to preserve the earth for the future generations. Other than hydro power, wind and photovoltaic energy holds the most potential to meet our energy demands. Alone, wind energy is capable of supplying large amounts of power but its presence is highly unpredictable as it can be here one moment and gone in another. Similarly, solar energy is present throughout the day but the solar irradiation levels vary due to sun intensity and unpredictable shadows cast by clouds, birds, trees, etc. The common inherent drawback of wind and photovoltaic systems are their intermittent natures that make them unreliable. However, by combining these two intermittent sources and by incorporating maximum power point tracking (MPPT) algorithms, the system's power transfer efficiency and reliability can be improved significantly when a source is unavailable or insufficient in meeting the load demands, the other energy source can compensate for the difference. Several hybrid wind/PV power systems with MPPT control have been proposed and discussed in works [1]- [5]. Most of the systems in literature use a separate DC/DC boost converter connected in parallel in the rectifier stage as shown in Figure 1 to perform the MPPT control for each of the renewable energy power sources [1]-[4]. A simpler multi input structure has been suggested by [5] that combine the sources from the DC-end while still achieving MPPT for each renewable source. The structure proposed by [5] is a fusion of the buck and buck-boost converter. The systems in literature require passive input filters to remove the high frequency current harmonics injected into wind turbine generators [6].The harmonic content in the generator current decreases its lifespan and increases the power loss due to heating [6]. In this paper, an alternative multi-input rectifier structure is proposed for hybrid wind/solar energy systems. The proposed design is a fusion of the Cuk and SEPIC converters. The features of the proposed topology are: 1) the inherent nature of these two converters eliminates the need for separate input filters for PFC [7]-[8]; 2) it can support step up/down operations for each renewable source (can support wide ranges of PV and wind input); 3) MPPT can be realized for each source; 4) individual and simultaneous operation is supported. The circuit operating principles will be discussed in this paper. Simulation results are provided to verify with the feasibility of the proposed system.

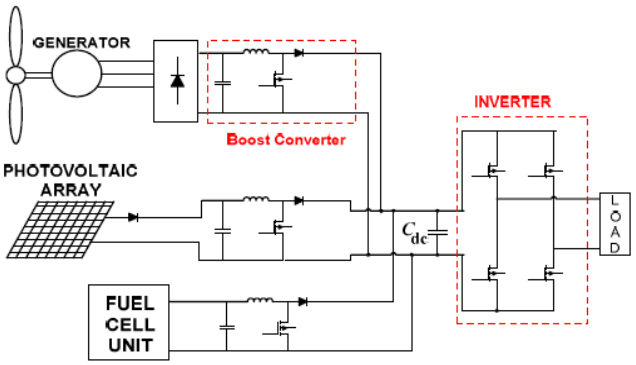


Fig. 1: Hybrid system with multi-connected boost converter

## 2. PROPOSED MULTI-INPUT RECTIFIER STAGE

A system diagram of the proposed rectifier stage of a hybrid energy system is shown in Figure 3, where one of the inputs is connected to the output of the PV array and the other input connected to the output of a generator. The fusion of the two converters is achieved by reconfiguring the two existing diodes from each converter and the shared utilization of the Cuk output inductor by the SEPIC converter. This configuration allows each converter to operate normally individually in the event that one source is unavailable. Figure 4 illustrates the case when only the wind source is available. In this case, *D*1 turns off and *D*2 turns on; the proposed circuit becomes a SEPIC converter and the input to output voltage relationship is given by (1). On the other hand, if only the PV source is available, then *D*2 turns off and *D*1 will always be on and the circuit becomes a Cuk converter as shown in Figure 5. The input to output voltage relationship is given by (2). In both cases, both converters have step-up/down capability, which provide more design flexibility in the system if duty ratio control is utilized to perform MPPT control.

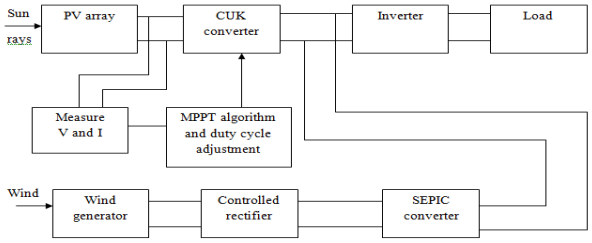


Fig.2 Block diagram of proposed system

$$\frac{V_{dc}}{V_W} = \frac{d_2}{1-d_2} \quad (1)$$

$$\frac{V_{dc}}{V_{PV}} = \frac{d_1}{1-d_1} \quad (2)$$

Figure 6 illustrates the various switching states of the proposed converter. If the turn on duration of *M*1 is longer than *M*2, then the switching states will be state I, II, IV. Similarly, the switching states will be state I, III, IV if the switch conduction periods are vice versa. To provide a better explanation, the inductor current waveforms of each switching state are given as follows assuming that $d2 > d1$; hence only states I, III, IV are discussed in this example. In the following, *Ii,PV* is the average input current from the PV source; *Ii,W* is the RMS input current after the rectifier (wind case); and *Idc* is the average system output current. The key waveforms that illustrate the switching states in this example are shown in Figure6. The mathematical expression that relates the total output voltage and the two input sources will be illustrated in the next section.

*State I ($M_1$ on, $M_2$ on):*

$$i_{L1} = I_{i,PV} + \frac{V_{PV}}{L_1} t \qquad 0 < t < d_1 T_s$$

$$i_{L2} = I_{dc} + \left(\frac{v_{c1}+v_{c2}}{L_2}\right) t \qquad 0 < t < d_1 T_s$$

$$i_{L3} = I_{i,W} + \frac{V_W}{L_3} t \qquad 0 < t < d_1 T_s$$

*State III (M1 off, M2 on) :*

$$i_{L1} = I_{i,PV} + \left(\frac{V_{PV} - v_{c1}}{L_1}\right) t \qquad d_1 T_s < t < d_2 T_s$$

$$i_{L2} = I_{dc} + \frac{v_{c2}}{L_2} t \qquad d_1 T_s < t < d_2 T_s$$

$$i_{L3} = I_{iW} + \frac{V_W}{L_3} t \qquad d_1 T_s < t < d_2 T_s$$

*State IV (M1 off, M2 off) :*

$$i_{L1} = I_{i,PV} + \left(\frac{V_{PV} - v_{c1}}{L_1}\right) t \qquad d_2 T_s < t < T_s$$

$$i_{L2} = I_{dc} - \frac{V_{dc}}{L_2} t \qquad d_2 T_s < t < T_s$$

$$i_{L3} = I_{iW} + \left(\frac{V_W - v_{c2} - V_{dc}}{L_3}\right) t \qquad d_2 T_s < t < T_s$$

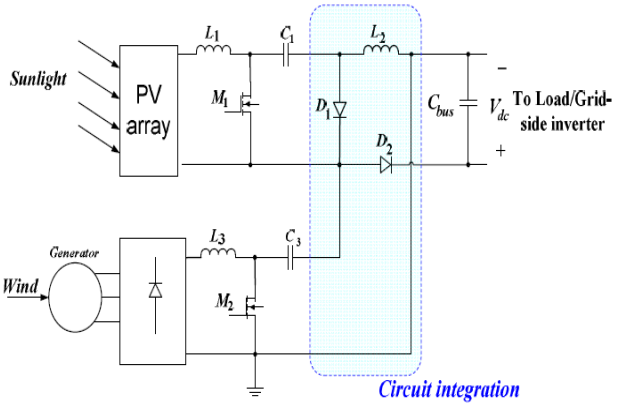


Fig. 3: Proposed rectifier stage for a Hybrid wind/PV system

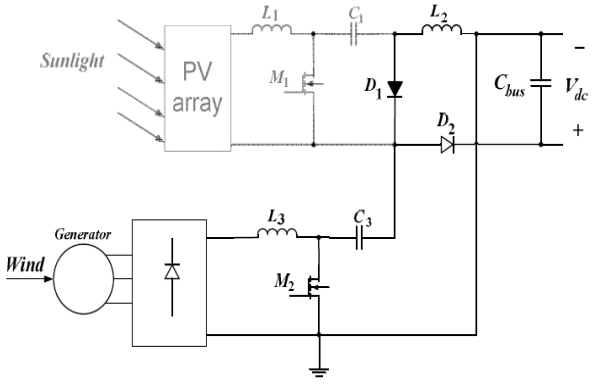


Fig.4 Only wind source is operational (SEPIC)

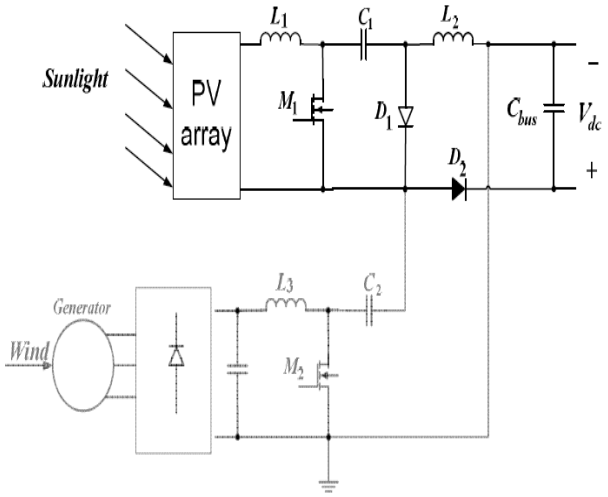


Fig.5 Only PV source is operation (Cuk)

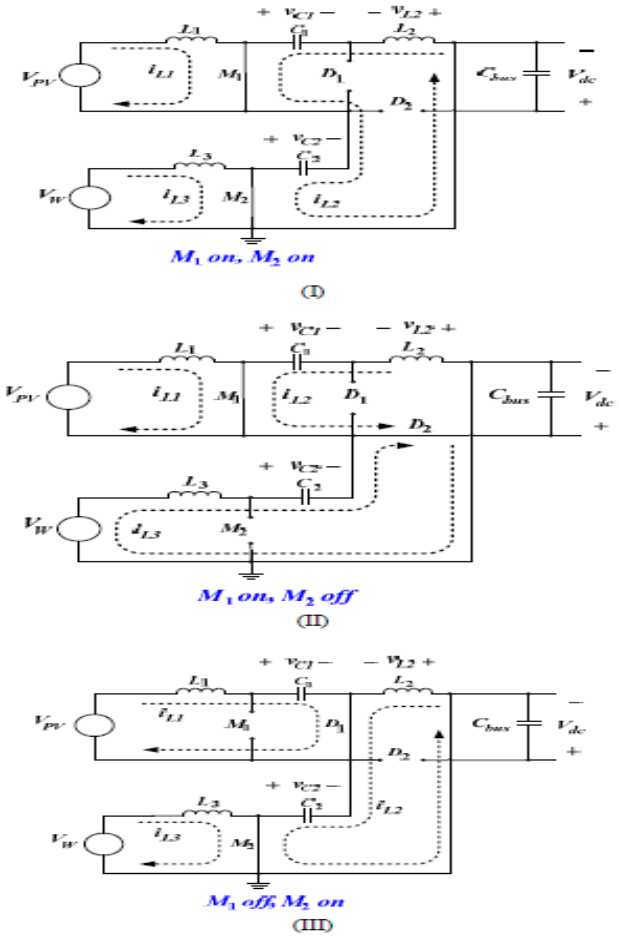


Fig.6 Switching states within a switching cycle

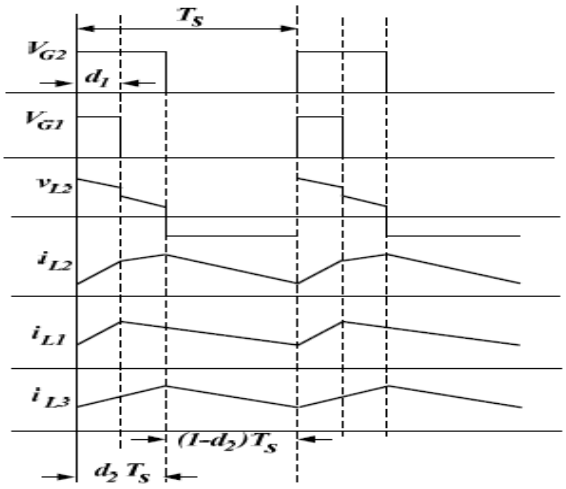


Fig.7 Proposed circuit inductor waveform

## 3. ANALYSIS OF PROPOSED CIRCUIT

To find an expression for the output DC bus voltage, *Vdc*, the volt-balance of the output inductor, *L*2, is examined according to Figure 6 with *d*2 > *d*1. Since the net change in the voltage of *L*2 is zero, applying volt-balance to *L*2 results in (3). The expression that relates the average output DC voltage (*Vdc*) to the capacitor voltages (*vc*1 and *vc*2) is then obtained as shown in (4), where *vc*1 and *vc*2 can then be obtained by applying volt-balance to *L*1 and *L*3 [9]. The final expression that relates the average output voltage and the two input sources ($V_W$ and $V_{PV}$) is then given by (5). It is observed that *Vdc* is simply the sum of the two output voltages of the Cuk and SEPIC converter. This further implies that *Vdc* can be controlled by *d*1 and *d*2 individually or simultaneously.

$$(v_{c1} + v_{c2})\, d_1\, T_s + (v_{c2})\, (d_2 - d_1)\, T_s + (1 - d_2)\, (-V_{dc}) T_s = 0 \quad (3)$$

$$V_{dc} = \left(\frac{d_1}{1-d_1}\right) v_{c1} + \left(\frac{d_2}{1-d_2}\right) v_{c2} \quad (4)$$

$$V_{dc} = \left(\frac{d_1}{1-d_1}\right) V_{PV} + \left(\frac{d_2}{1-d_2}\right) V_W \quad (5)$$

The switches voltage and current characteristics are also provided in this section. The voltage stress is given by (6) and (7) respectively. As for the current stress, it is observed from figure 6 that the peak current always occurs at the end of the on-time of the MOSFET. Both the Cuk and SEPIC MOSFET current consists of both the input current and the capacitors (*C*1 or *C*2) current. The peak current stress of *M*1 and *M*2 are given by (8) and (10) respectively. *Leq*1 and *Leq*2, given by (9) and (11), represent the equivalent inductance of Cuk and SEPIC

converter respectively. The PV output current, which is also equal to the average input current of the Cuk converter is given in (12). It can be observed that the average inductor current is a function of its respective duty cycle ($d1$). Therefore by adjusting the respective duty cycles for each energy source, maximum power point tracking can be achieved.

$$v_{ds1} = V_{pv}\left(1 + \frac{d_1}{1- d_1}\right) \quad (6)$$

$$v_{ds2} = V_W\left(1 + \frac{d_2}{1- d_2}\right) \quad (7)$$

$$i_{ds1,pk} = I_{i,PV} + I_{dc,avg} + \frac{V_{PV}\, d_1\, T_S}{2L_{eq1}} \quad (8)$$

$$L_{eq1} = \frac{L_1\, L_2}{L_1 + L_2} \quad (9)$$

$$i_{ds2,pk} = I_{i,W} + I_{dc,avg} + \frac{V_W\, d_2\, T_S}{2L_{eq2}} \quad (10)$$

$$L_{eq2} = \frac{L_3\, L_2}{L_3 + L_2} \quad (11)$$

$$I_{i,PV} = \frac{P_0}{V_{dc}}\,\frac{d_1}{1- d_1} \quad (12)$$

## 4. MPPT CONTROL OF PROPOSED CIRCUIT

A common inherent drawback of wind and PV systems is the intermittent nature of their energy sources. Wind energy is capable of supplying large amounts of power but its presence is highly unpredictable as it can be here one moment and gone in another. Solar energy is present throughout the day, but the solar irradiation levels vary due to sun intensity and unpredictable shadows cast by clouds, birds, trees, etc.These drawbacks tend to make these renewable systems inefficient. However, by incorporating maximum power point tracking (MPPT) algorithms, the systems' power transfer efficiency can be improved significantly.to describe a wind turbine's power characteristic, equation (13) describes the mechanical power that is generated by the wind [6].

$$p_m = 0.5\rho A\, C_p\,(\lambda, \beta)\mathrm{v}_\mathrm{w}^3 \quad (13)$$

*Where*

*ρ = air density,*

*A = rotor swept area,*

*Cp(λ, β) = power coefficient function*

*λ =tip speed ratio,*

*β = pitch angle,*

*vw = wind speed*

The power coefficient (Cp) is a nonlinear function that represents the efficiency of the wind turbine to convert wind energy into mechanical energy. It is dependent on two variables, the tip speed ratio (TSR) and the pitch angle. The TSR, λ, refers to a ratio of the turbine angular speed over the wind speed. The mathematical representation of the TSR is given by (14) [10]. The pitch angle, β, refers to the angle in which the turbine blades are aligned with respect to its longitudinal axis.

$$\lambda = \frac{R\,\omega_b}{v_w} \quad (14)$$

*Where*

*R = turbine radius,*

*ωb = angular rotational speed*

Figure 8 and 9 are illustrations of a power coefficient curve and power curve for a typical fixed pitch ($\beta$ =0) horizontal axis wind turbine. It can be seen from figure 8 and 9 that the power curves for each wind speed has a shape similar to that of the power coefficient curve. Because the TSR is a ratio between the turbine rotational speed and the wind speed, it follows that each wind speed would have a different corresponding optimal rotational speed that gives the optimal TSR. For each turbine there is an optimal TSR value that corresponds to a maximum value of the power coefficient (Cp,max) and therefore the maximum power. Therefore by controlling rotational speed, (by means of adjusting the electrical loading of the turbine generator) maximum power can be obtained for different wind speeds.

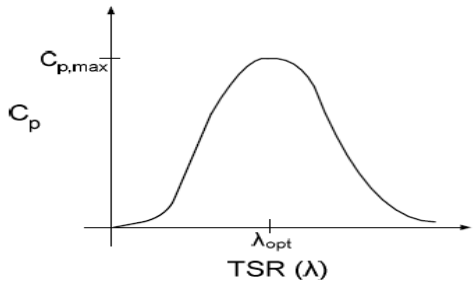


Fig 8: Power Coefficient Curve for a typical wind turbine

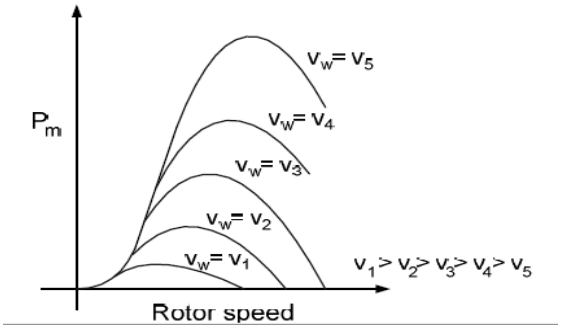


Fig 9:Power Curves for a typical wind turbine

A solar cell is comprised of a P-N junction semiconductor that produces currents via the photovoltaic effect. PV arrays are constructed by placing numerous solar cells connected in series and in parallel [5]. A PV cell is a diode of a large-area forward bias with a photovoltage and the equivalent circuit is shown by Figure 10 [11]. The current-voltage characteristic of a solar cell is derived in [12] and [13] as follows

$$I = I_{ph} - I_D \quad (15)$$

$$I = I_{ph} - I_0 \left[\exp\left(\frac{q(V+R_S I)}{A\,k_B\,T}\right) - 1\right] - \frac{V+R_S\,I}{R_{sh}} \quad (16)$$

*Where*

*Iph = photocurrent*

*ID = diode current,*

*I0 = saturation current,*

*A = ideality factor,*

*q = electronic charge 1.6x10-9,*

*kB = Boltzmann's gas constant (1.38x10-23),*

*T = cell temperature,*

*Rs = series resistance,*

*Rsh = shunt resistance,*

*I = cell current,*

*V = cell voltage*

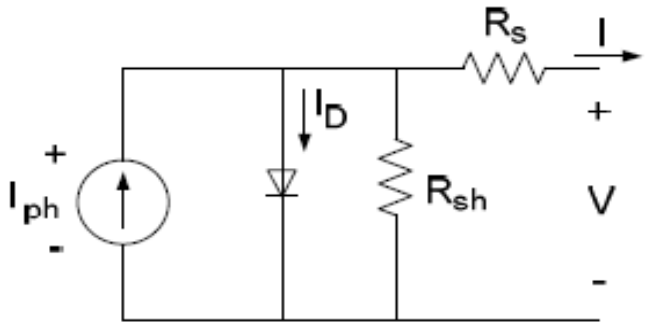


Fig.10: PV cell equivalent circuit

Typically, the shunt resistance (Rsh) is very large and the series resistance (Rs) is very small [5]. Therefore, it is

common to neglect these resistances in order to simplify the solar cell model. The resultant ideal voltage-current

characteristic of a photovoltaic cell is given by (17) and illustrated by Figure 11. [5]

$$I = I_{ph} - I_0 \left(\exp\left(\frac{qV}{kT}\right) - 1\right) \quad (17)$$

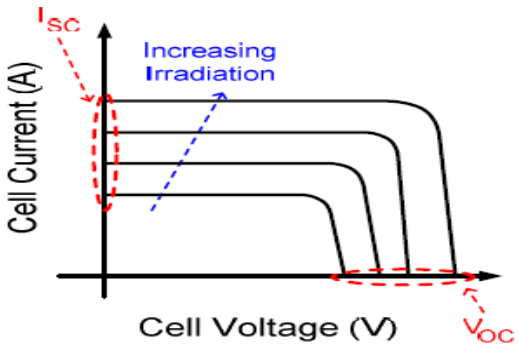


Fig 11: PV cell voltage-current characteristic

The typical output power characteristics of a PV array under various degrees of irradiation is illustrated by Figure 11. It can be observed in Figure 12 that there is a particular optimal voltage for each irradiation level that corresponds to maximum output power. Therefore by adjusting the output current (or voltage) of the PV array, maximum power from the array can be drawn.

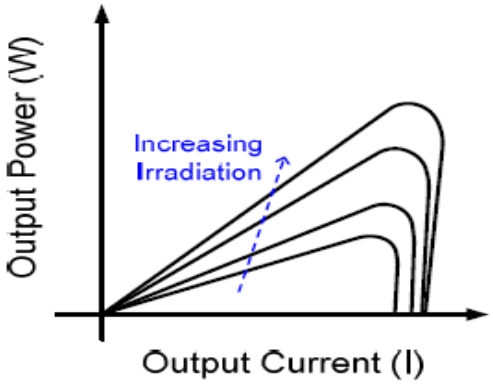


Fig 12: PV cell power characteristics

Due to the similarities of the shape of the wind and PV array power curves, a similar maximum power point tracking scheme known as the hill climb search (HCS) strategy is often applied to these energy sources to extract maximum power. The HCS strategy perturbs the operating point of the system and observes the output. If the direction of the perturbation (e.g an increase or decrease in the output voltage of a PV array) results in a positive change in the output power, then the control algorithm will continue in the direction of the previous perturbation. Conversely, if a negative change in the output power is observed, then the control algorithm will reverse the direction of the pervious perturbation step. In the case that the change in power is close to zero (within a specified range) then the algorithm will invoke no changes to the system operating point since it corresponds to the maximum power point (the peak of the power curves). The MPPT scheme employed in this paper is a version of the HCS strategy. Figure 13 is the flow chart that illustrates the implemented MPPT scheme.

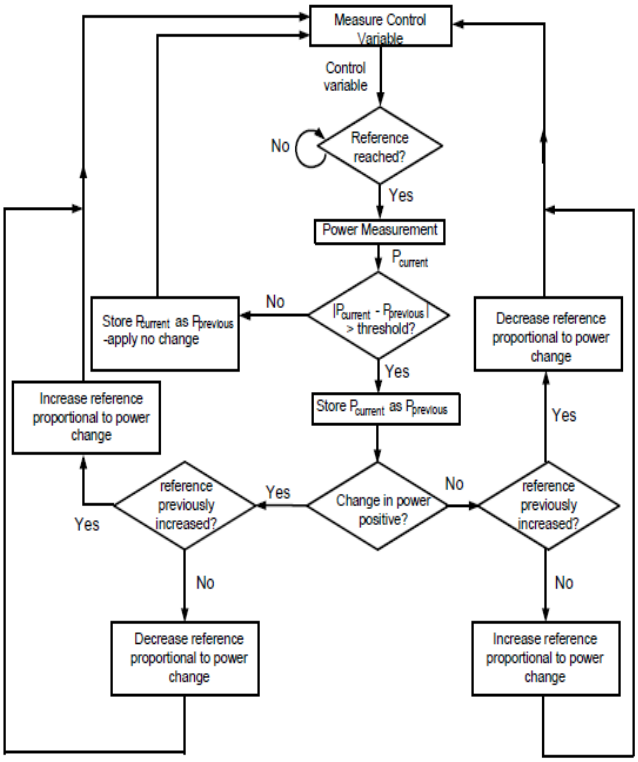


Fig. 13: General MPPT Flow Chart for wind and PV

## 5. SIMULATION RESULTS

The simulation has been conducted for the above models in MATLAB. The analysis for the same has been described as below. Here Case I illustrates the simultaneous operation (Cuk-SEPIC fusion mode) of the two sources where M2 has a longer conduction cycle. In Case II the system under the condition where the wind source has failed and only the PV source (Cuk converter mode) is supplying power to the load. Whereas in case III the system where only the wind turbine generates power to the load (SEPIC converter mode).

CASE I: - Simultaneous operation with both wind and PV source (Fusion mode with Cuk and SEPIC)

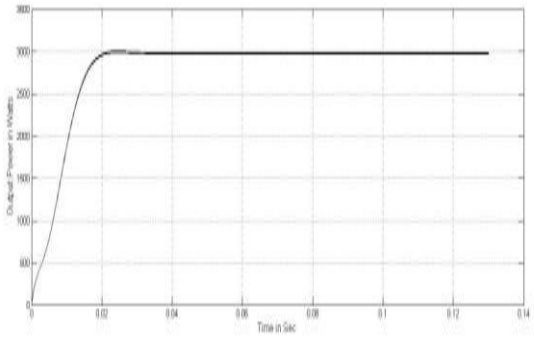

Fig 13: Output Power with both wind and PV source

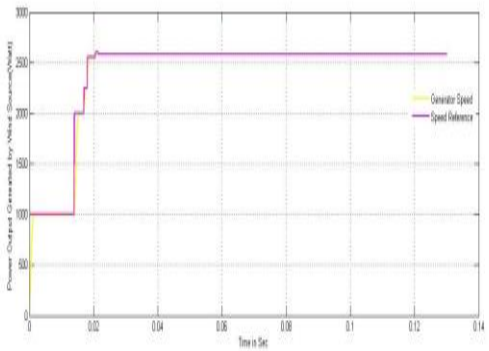

Fig 14:- Wind MPPT – Generator speed and reference speed signal(SEPIC operation)

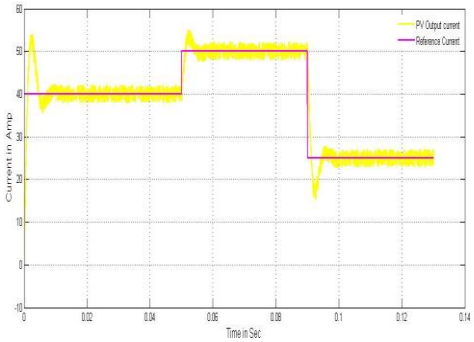


Fig 15:- Solar MPPT – PV output current and reference current signal (Cuk operation)

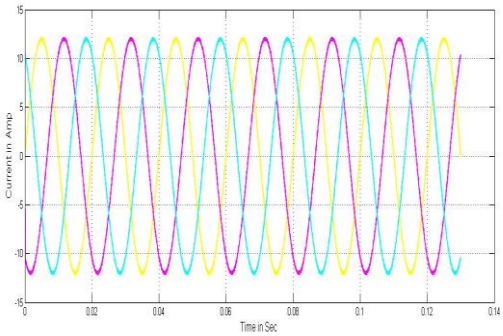


Fig 16:- The injected three phase generator current

From the above figure 13, it can be seen that when simultaneous operation of Wind & PV source is running the output power is in the range of 2.98kW (approx 3kW). Both the MPPT controller works simultaneously & follows the reference signal in order to have maximum power output. The operation of the PV component of the system (Cuk operation) and the Wind component of the system (SEPIC operation) is shown in Fig 14 & Fig 15 respectively.

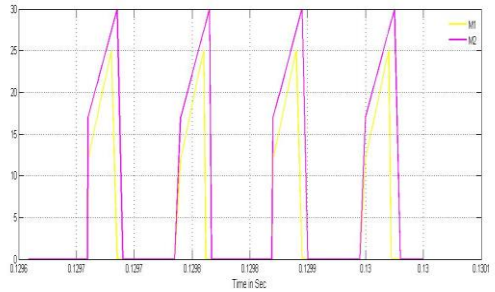


Fig 17: Switch currents (M1 and M2) during Simultaneous operation with both wind and PV source (Fusion mode with Cuk and SEPIC)

From the above figure 16 the current injected by the wind generator has been shown which indicate the contribution of Wind source towards interconnected grid. Fig 17 indicates the MosFET switch currents in CUK & SEPIC converter during Simultaneous operation with both wind and PV source (Fusion mode with Cuk and SEPIC). In this case the circuit operates in converter states I, IV and III. The switch M2 conducts for longer duration of cycle compared with M1.

CASE II: - Individual operation with only PV source (Cuk operation)

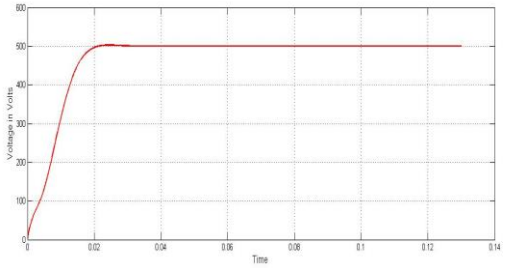


Fig 18: Output Voltage with only PV source

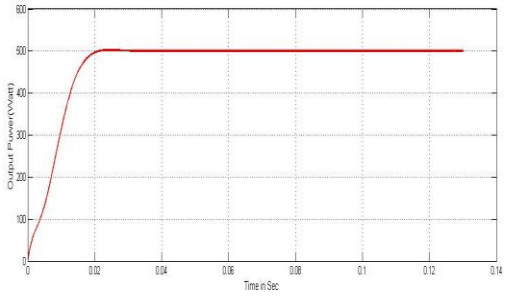


Fig 6.7: Output Power with only PV source

From the above figure 18 & 19, it can be seen that wind source has failed and only the PV source (Cuk converter mode) is supplying power to the load. Output power delivered is in the range of 0.5kW at 500V. Only solar MPPT controller works to have maximum power output.

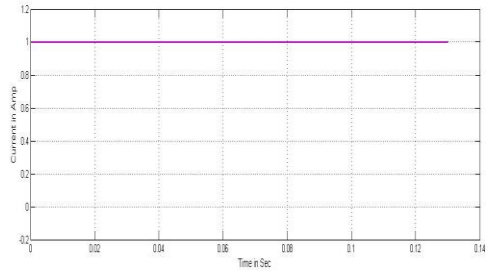


Fig 19: Output Current of PV source

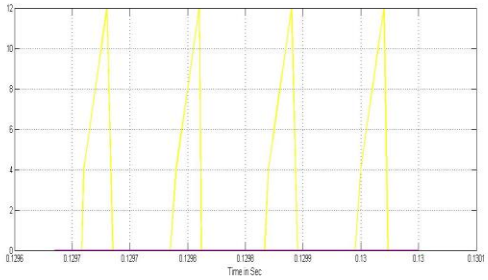


Fig 20:- Switch currents (M1 and M2) with only PV source

From the above figure the current injected by the PV source has been shown which indicate the contribution of PV source towards interconnected grid. Fig indicates the MosFET switch M1 & M2 currents in CUK & SEPIC converter. As wind source has failed only M1 is conducting & M2 is OFF & circuit is working in CUK mode.

CASE III: - Individual operation with only Wind source (SEPIC operation)

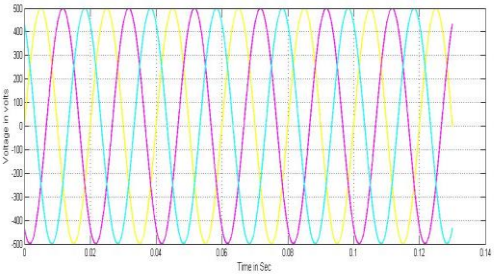


Fig 21:- Output voltage with only Wind source

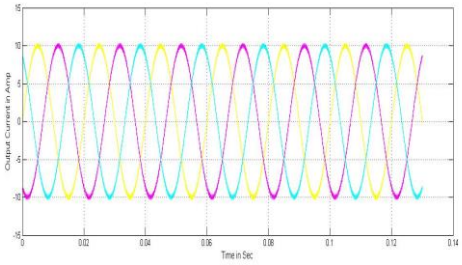


Fig 22:- Output current with only Wind source

From the above figure 21 & 22, it can be seen that PV source has failed and only the wind source (SEPIC converter mode) is supplying power to the load. Output power delivered is in the range of 1.8kW at 500V. Only Wind MPPT controller works to have maximum power output.

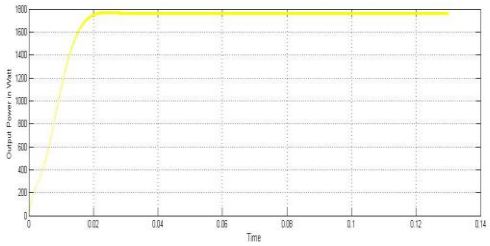

Fig23:- Output Power with only Wind source

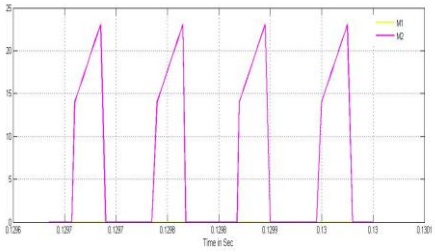

Fig 24:- Switch currents (M1 and M2) with only Wind source

From the above figure 23 the current injected by the Wind source has been shown which indicate the contribution of wind source towards interconnected grid. Fig 24 indicates the MosFET switch M1 & M2 currents in CUK & SEPIC converter. As Solar source has failed only M2 is conducting & M1 is OFF & circuit is working in SEPIC mode. The result discussed above has been tabulated to conclude the performance of the CUK-SEPIC Converter for Hybrid System.

Design specifications:

| | |
|---|---|
| Output Power | 3KW |
| Output voltage | 500V |
| Switching Frequency | 20 KHz |

## 6. CONCLUSION & FUTURE SCOPE

### Conclusion

A new multi-input CUK-SEPIC rectifier stage for hybrid wind/solar energy systems has been presented. Additional input filters are not necessary to filter out high frequency harmonics. Both renewable sources can be stepped up/down (supports wide ranges of PV and wind input). MPPT can be realized for each source. Individual and simultaneous operation is supported.

### Future Scope

- A hardware system can be implemented to visualize the theoretical concepts presented in the above study.
- After the hardware implementation difficulties or any improvements required can be implemented in the proposed model to make it more accurate.

A comparative analysis on certain performance parameters can be made for the different converter circuits (like Buck/Boost) for same system & problems.

## REFERENCES

[1] S.K. Kim, J.H Jeon, C.H. Cho, J.B. Ahn, and S.H. Kwon, "Dynamic Modeling and Control of a Grid-Connected Hybrid Generation System with Versatile Power Transfer," *IEEE Transactions on Industrial Electronics*, vol. 55, pp. 1677-1688, April 2008.

[2] D. Das, R. Esmaili, L. Xu, D. Nichols, "An Optimal Design of a Grid Connected Hybrid Wind/Photovoltaic/Fuel Cell System for Distributed Energy Production," *in Proc. IEEE Industrial Electronics Conference*, pp. 2499-2504, Nov. 2005.

[3] N. A. Ahmed, M. Miyatake, and A. K. Al-Othman, "Power fluctuations suppression of stand-alone hybrid generation combining solar photovoltaic/wind turbine and fuel cell systems," *in Proc. Of Energy Conversion and Management, Vol. 49, pp. 2711-2719, October 2008.*

[4] S. Jain, and V. Agarwal, "An Integrated Hybrid Power Supply for Distributed Generation Applications Fed by Nonconventional Energy Sources," *IEEE Transactions on Energy Conversion, vol. 23, June 2008.*

[5] Y.M. Chen, Y.C. Liu, S.C. Hung, and C.S. Cheng, "Multi-Input Inverter for Grid-Connected Hybrid PV/Wind Power System," *IEEE Transactions on Power Electronics*, vol. 22, May 2007.

[6] dos Reis, F.S., Tan, K. and Islam, S., "Using PFC for harmonic mitigation in wind turbine energy conversion systems" *in Proc. of the IECON 2004 Conference*, pp. 3100- 3105, Nov. 2004.

[7] R. W. Erickson, "Some Topologies of High Quality Rectifiers" *in the Proc. of the First International Conference on Energy, Power, and Motion Control*, May 1997.

[8] D. S. L. Simonetti, J. Sebasti´an, and J. Uceda, "The Discontinuous Conduction Mode Sepic and ´ Cuk Power Factor Preregulators: Analysis and Design" *IEEE Trans. On Industrial Electronics*, vol. 44, no. 5, 1997

[9] N. Mohan, T. Undeland, and W Robbins, "Power Electronics: Converters, Applications, and Design," John Wiley & Sons, Inc., 2003.

[10] J. Marques, H. Pinheiro, H. Grundling, J. Pinheiro, and H. Hey, "A Survey on Variable-Speed Wind Turbine System," Proceedings of Brazilian Conference of Electronics of Power, vol. 1, pp. 732-738, 2003.

[11] F. Lassier and T. G. Ang, "Photovoltaic Engineering Handbook" 1990

[12] Global Wind Energy Council (GWEC), "Global wind 2008 report,"June 2009.

[13] L. Pang, H. Wang, Y. Li, J. Wang, and Z. Wang, "Analysis of Photovoltaic Charging System Based on MPPT," Proceedings of Pacific-Asia Workshop on Computational Intelligence and Industrial Application 2008 (PACIIA '08), Dec 2008, pp. 498-501.

[14] "A Hybrid Wind-Solar Energy System: A New Rectifier Stage Topology" Joanne Hui*, IEEE Student Member, Alireza Bakhshai, IEEE Senior Member, and Praveen K. Jain, IEEE Fellow Department of Electrical and Computer Engineering Queen's Center for Energy and Power Electronics Research (ePOWER), Queen's University Kingston, Ontario, Canada*email: 2cyjh@queensu.ca

[15] A PHOTOVOLTAIC PANEL MODEL IN MATLAB/SIMULINK Shivananda Pukhrem* shivananda.pukhrem@yahoo.com,196409 @student.pwr.wroc.pl Faculty of Electrical Engineering Program: Renewable Energy System Wroclaw University of Technology, 27 Wybrzeże Wyspiańskiego St., 50-370 Wrocław, Poland

[16] A CUK-SEPIC FUSED CONVERTER TOPOLOGY FOR WIND-SOLAR HYBRID SYSTEMS FOR STAND-ALONE SYSTEMS

[17]SURESH K V*, VINAYAKA K U**, RAJESH U** * PG Student, Department of EEE, SIT, Tumkur, India, srshkumar94@gmail.com **Asst. Prof., Department of EEE, SIT, Tumkur, India,vinay.ene@gmail.com **Asst. Prof., Department of EEE, SIT, Tumkur, India,u.rajesheee@gmail.com International Journal of Emerging Technology in Computer Science & Electronics (IJETCSE) ISSN: 0976-1353 Volume 14 Issue 2 –APRIL 2015

[18]INTEGRATION OF CUK AND SEPIC CONVERTERS FOR HYBRID RENEWABLE ENERGY SYSTEMS Dharani.M, K.Rajalashmi, Dr.S.U.Prabha, K. Indu Rani Department of Electrical And Electronics Engineering, Bannari Amman Institute of Technology, *Sathyamangalam Corresponding Author: Dharani.M E-mail:dharanimoorthi@gmail.com South Asian Journal of Engineering and Technology Vol.2, No.16(2016)*